Nano–porous pyrite and organic matter in 3.5-billion-year-old stromatolites record primordial life

Raphael J. Baumgartner[1], Martin J. Van Kranendonk[1], David Wacey[2], Marco L. Fiorentini[3], Martin Saunders[2], Stefano Caruso[3], Anais Pages[4], Martin Homann[5] and Paul Guagliardo[3]

[1]Australian Centre for Astrobiology, School of Biological, Earth and Environmental Sciences, University of New South Wales, Kensington, New South Wales 2052, Australia
[2]Centre for Microscopy, Characterization and Analysis, University of Western Australia, Perth, Western Australia 6009, Australia [3]Centre for Exploration Targeting, School of Earth Sciences, University of Western Australia, Perth, Western Australia 6009, Australia [4]Commonwealth Scientific and Industrial Research Organization, Mineral Resources, Kensington, Western Australia 6151, Australia [5]European Institute for Marine Studies, CNRS–UMR6538, Laboratoire Géosciences Océan, Technopôle Brest–Iroise, Plouzané 29280, France

Geological Society of America | GEOLOGY | https://doi.org/10.1130/G46365.1
Manuscript received 9 April 2019 Revised manuscript received 30 July 2019 Manuscript accepted 9 August 2019

ABSTRACT

Stromatolites of the ~3.5 billion-year-old Dresser Formation (Pilbara Craton, Western Australia) are considered to be some of Earth's earliest convincing evidence of life. However, uniquely biogenic interpretations based on surface outcrops are precluded by weathering, which has altered primary mineralogy and inhibited the preservation of microbial remains. Here, we report on exceptionally preserved, strongly sulfidized stromatolites obtained by dia- mond drilling from below the weathering profile. These stromatolites lie within undeformed hydrothermal-sedimentary strata and show textural features that are indicative of biogenic origins, including upward-broadening and/or upward-branching digitate forms, wavy to wrinkly laminae, and finely laminated columns that show a thickening of laminae over flex- ure crests. High-resolution textural, mineralogical, and chemical analysis reveals that the stromatolites are dominated by petrographically earliest, nano-porous pyrite that contains thermally mature, N-bearing organic matter (OM). This nano-porous pyrite is consistent with a formation via sulfidization of an originally OM-dominated matrix. Evidence for its relationship with microbial communities are entombed OM strands and filaments, whose microtexture and chemistry are consistent with an origin as mineralized biofilm remains, and carbon isotope data of extracted OM ($^{TM13}C_{OM} = -29.6‰ \pm 0.3‰$ VPDB [Vienna Peedee belemnite]), which lie within the range of biological matter. Collectively, our findings pro- vide exceptional evidence for the biogenicity of some of Earth's oldest stromatolites through preservation of OM, including microbial remains, by sulfidization.

INTRODUCTION

Some of the oldest, best–preserved stromat- olites of probable biogenic origin are from the ca. 3481 ± 2 Ma North Pole Chert Member of the Dresser Formation, Pilbara Craton, West- ern Australia (Walter et al., 1980; Buick et al., 1981; Groves et al., 1981; Schopf et al., 2006; Van Kranendonk, 2006, 2011; Van Kranendonk et al., 2008). This hydrothermal−sedimentary unit, which has experienced only low-grade metamorphism (prehnite-pumpellyite to low- ermost greenschist facies conditions; Dunlop and Buick, 1981; Terabayashi et al., 2003; Van Kranendonk and Pirajno, 2004), hosts stromato- lites that are interbedded with metasedimentary rocks displaying primary textures such as ripple marks, desiccation cracks, and aragonite crystal splays now altered to secondary phases. These characteristics, together with the presence of hydrothermal chert-barite and geyserite, indi- cate a shallow marine to subaerial depositional environment that was influenced by hydrother- mal activity (Walter et al., 1980, Groves et al., 1981; Buick et al., 1981; Buick and Dunlop, 1990; Van Kranendonk, 2006, 2011; Van Kranendonk et al., 2008; Djokic et al., 2017; Otálora et al., 2018).

These studies interpreted a biogenic origin for the stromatolites on basis of (1) their geological and stratigraphical context, (2) their morphological expression, including the pres- ence of wrinkly laminations, and (3) their rela- tion to sedimentary bedding. Biologically medi- ated origins are indirectly supported by carbon isotope data of rare OM occurrences (Ueno et al., 2001; Morag et al., 2016), and sulfur isotopic analyses of barite-pyrite assemblages elsewhere in the Dresser Formation (Shen et al., 2001, 2009; Ueno et al., 2008). Previous studies, however, have failed to uncover microbial re- mains and diagnostically biogenic microfossils, and a biogenic interpretation of the stromatolites has been controversial because of studies show- ing abiogenic formation of stromatolite-like textures (e.g., Grotzinger and Rothman, 1996; McLoughlin et al., 2008).

Here, we present the results from a detailed microanalytical examination of exceptionally preserved, strongly sulfidized Dresser Forma- tion stromatolites sampled from a drill core from below the effects of surface weathering. We used a multi-technique analytical approach comprising (1) scanning electron microscopy (SEM) and scanning transmission electron mi- croscopy (STEM) combined with energy dis- persive X–ray spectroscopy (EDS) analysis; (2) Raman spectroscopy analysis; (3) ion mapping by nano-

scale secondary ion mass spectrom- etry (NanoSIMS); and (4) stable carbon isotope analysis of extracted OM. Our results reveal that the Dresser Formation stromatolites are dominantly composed of frameworks of nano− porous pyrite that contains widespread inclu- sions of N-bearing OM, as well as OM strands and filaments that closely resemble remnants of biofilms.

SAMPLE MATERIALS AND METHODS

Sample materials were obtained from a drill core collected in 2004 from the North Pole Chert Member of the Dresser Formation (Fig. DR1 in the GSA Data Repository[1]). Details on the geol- ogy and stratigraphy of the drill core (PDP2b; GPS coordinates 75°22′46″N, 76°56′26″E), as well as the spatial correlation of the contained stromatolite structures to their equivalents at the surface, are reported by Van Kranendonk et al. (2008). For this study, two slices of stromato- lites were cut and placed into two polished thin sections (sample S1; Fig. 1A; Fig. DR2a), and into one polished epoxy mount and one thin sec- tion (sample S2; Figs. DR2b and DR2c). The remaining sample materials were subjected to bulk rock organic carbon isotope analysis. The mineralogy and chemistry of sulfides within the stromatolites have been examined by SEM and EDS analysis. This work was done both prior to, and after, nitric acid treatment, which dissolves sulfide phases and exposes OM. Prior to nitric acid etching, ion maps of $^{16}O^-$, $^{12}C^-$, $^{26}CN^-$, and $^{58}Ni^+$ were obtained using NanoSIMS analysis. In addition, wafers of sulfide were prepared us- ing focused ion beam milling, and thereafter subjected to STEM analysis. Raman spectroscopy analysis of OM was carried out on un- etched and etched sample surfaces. See the Data Repository for full method details.

RESULTS

Stromatolite Textures and Micro-Mineralogy of Sulfide

The stromatolites occur within centimeters- thick, planar chert-dolomite horizons that are flanked by layers of coarsely crystalline, hy- drothermal barite (Fig. 1; Fig. DR2). The stro- matolites are composed dominantly of sulfide, together with dolomite and chert. In sample S1, columnar stromatolites consist of upward- broadening and/or upward-branching digitate structures that are overlain by centimeter-size caps of submillimeter scale, wavy to undu- lating and wrinkly, laminae that occasionally span individual columns (Fig. 1; Fig. DR2a). The stromatolites are cut by barite veins that are barren in sulfides (Fig. 1A; Fig. DR2a). Sample S2, which lacks digitate structures, is composed of laterally continuous to discontinuous, wavy laminae, and irregular- to finely laminated col- umns (Figs. DR2b– DR2d).

The stromatolites dominantly consist of pyrite, but also contain subordinate sphalerite, millerite, and galena. High-resolution SEM and STEM analysis revealed three main pyrite gen- erations (Figs. 2A–2C; Fig. DR3). The earliest generation of irregular nano-porous pyrite (Py1) comprises anhedral to rounded pyrite grains, usually <0.1–1 µm in diameter. Interestingly,

nano-scale porosity is also present in associ- ated sphalerite, millerite, and galena (Figs. DR3d–DR3f, and DR4a). Zoned nano-porous pyrite (Py2) typically mantles Py1. It exhibits concentric banding defined by nano-scale poros- ity, and shows pseudo-grain boundaries lined by void trails. The assemblages of Py1 and Py2, which are overgrown by non-porous, massive pyrite (Py3), form distinctly vertical, upward- broadening and/or upward-branching patterns within the digitate structures (Fig. 2D), but a more irregular framework within the layered stromatolites (Fig. 2E).

Organic Matter in Sulfide

NanoSIMS ion mapping and Raman spec- troscopy analysis indicate that Py1 and Py2 are enriched in Ni and host thermally mature, N-bearing OM (CN_{org} in NanoSIMS analysis; Fig. 3; Fig. DR4). This OM is interpreted to reside in the nano-pores and void spaces of Py1 and Py2. The relative heights and shapes of disorder-induced 'D' (~1315 Δcm^{-1}) and or- der-induced 'G' (~1600 Δcm^{-1}) Raman bands of the OM are consistent with literature data of thermally mature Archean OM elsewhere in the Dresser Formation (Harris et al., 2015). This characteristic precludes an origin of OM in the stromatolites from post–metamorphic contamination. The bulk OM extracted from a millimeter-thick volume cut from sample S2 yields 0.3% total organic carbon (TOC) with a $\delta^{13}C_{OM}$ value of −29.6 ± 0.3‰ (VPDB [Vienna Peedee belemnite]). This value, which is with- in the range of previous data from the Dresser Formation (OM in bedded chert with –33.6‰ to –25.7 ‰ $\delta^{13}C_{OM}$; Morag et al., 2016), is typi- cal of biomass derived from microorganisms, although similar values have also been reported from abiotic OM synthesis (McCollom and Seewald, 2006). Nitric acid etching revealed that the OM within pyrite mostly occurs as irregular masses that are speckled by barite and calcite grains (Figs.DR5a and DR5b). It also forms complexly twisted, rope-like filaments that are usually <1 µm in diameter, as well as occasionally sinusoidal, axially arranged, partially calcified strands that reach lengths of up to ~20 µm (Fig. 4; Figs.DR5c–DR5d, DR6, and DR7). These OM filaments and strands are clearly embedded within Py1 and pass across grain boundaries of Py2 (Figs. 4A and 4B; Fig. DR5c and DR5d). The intimate association of these OM structures with pyrite, in addition to Raman Spectroscopy signatures that are equivalent to OM in unetched sulfide (Figs. 3E and 3F), indicate that the strands and filaments are autochthonous, and that they have not been altered substantially through nitric acid etching.

DISCUSSION

The undeformed und weakly metamor- phosed Dresser Formation stromatolites ex- amined in this study meet many of the textural criteria for stromatolite biogenicity (e.g., Buick et al., 1981; Walter, 1983; Awramik and Grey, 2005): they are syndepositional structures; they have grown perpendicular to bedding as finely laminated columns and as branching digitate structures; they exhibit wavy to wrinkly lami- nae, including laminae that thicken over crestal regions, and laminae at column margins that show near vertical inclination, as is consistent with them representing the remains of cohesive microbial mats (Fig. 1A). However, the stromatolites lack diagnostic evidence for trapped clastic grains, or syn-sedimentary deformational features requiring coherence mediated by flexible microbial mats (e.g., Grotzinger and Knoll, 1999; Allwood et al., 2009). In spite of such ambiguities, which have led to mistrust of textural biosignatures (e.g., Lowe, 1994; Neveu et al., 2018), our study demonstrates that the Dresser Formation stromatolites are composed of putative biomarker assemblages; i.e., petrographically earliest, organic matter–rich nanoporous pyrite that hosts probable microbial remains.

In general, the formation of OM-rich nano-porous pyrite, which forms the bulk of the stromatolites studied here, requires the presence of abundant OM during sulfidization. For exam- ple, it is known from OM-rich shales (Cui et al., 2018), pyritized microfossils (Wacey et al., 2014), and biologically precipitated pyrite framboids, where it is represented by pyritized exopolymeric substance (EPS) mantling pyrite grains (Wacey et al., 2015). Crucially, the EPS of biofilms pro- vides the conditions required for Fe and S saturation, and establishes confined growth spaces that control the formation of rounded grains (MacLean et al., 2008; Wacey et al., 2015). Whereas regularly structured, equigranular, framboidal pyrite is not observed in this study, we note the presence of anhedral to rounded nano–scale py- rite grains embedded within, or mantled by, OM- rich nano-porous pyrite (Figs. 2B and 2C). Hence, Py1 within the stromatolites could have formed as early as during microbial growth, through sulfidization of EPS or degrading biomass. In con- trast, Py2 and Py3 may relate to later episodes of hydrothermal influence, which is consistent with late–stage barite veins cutting across the stromatolites (Fig. 1A; Fig. DR2a).

Early–stage sulfidization of microbial bio- mass is supported by the presence of coherent OM strands and filaments within Py1 and Py2 (Fig. 4; Figs. DR5c, DR5d, and DR7). Their textural diversity and viscoelastic properties, as ascertained from complex twisting and bundling, are similar to the rheological characteristics of EPS in biofilms. Whereas crudely reminiscent features have been produced in abiotic laboratory experiments (e.g., Cosmidis and Templeton, 2016), several differences distinguish them from the OM structures described here: (1) smaller diameters, in the range of few tens of nanometers; (2) more rigidness and less flexibility, expressed by filaments up to tens of microns in length with- out significant flexure or sinuosity; (3) the absence of complex twisting, bundling, and internal striation. In addition, the OM strands and filaments are not only carbonized and pyritized, but also calcified. This characteristic, plus the fact that calcite is only present in the stromatolites where there is OM, is consistent with calcification of EPS in biofilms, where negative charging of cellular matter attracts Ca^{2+} to stimulate calcite precipitation (Riding, 2000). Collectively, the abundance, texture, and chemistry of the OM, in addition to enrichments of N—a crucial requisite for functional groups of biomolecules—and $\delta^{13}C$ that overlaps the array of biotic origin, strongly suggests that it represents the remains of biofilms. Indeed, the axial and twisted arrangement of some later- ally continuous, sinusoidal, finely striated OM strands is reminiscent of EPS sheaths wrapped around filamentous bacteria, which break, un- furl, fray at the edges, and collapse into flattened elongate strands upon degradation (compare Figures 4B and 4C and Fig. DR7 with Planavsky et al. [2009, their figure 6], and Sprachta et al. [2001, their figure 14]). Irrespective of this de- tailed interpretation, the preservation of these delicate OM structures indicates rapid entombment by sulfidization as early as during stromatolite construction. It remains to be determined whether the precipitation of pyrite was mediated by metabolic reactions, such as microbial sulfate reduction producing H_2S, evidence for which has been reported from pyrite elsewhere in the Dresser Formation (Shen et al., 2001, 2009; Ueno et al., 2008).

CONCLUSION

Our detailed study of strongly sulfidized stromatolites within hydrothermal–sedimentary strata of the ~3.5 Ga Dresser Formation demonstrates that they are dominated by frameworks of nano–porous pyrite enriched in thermally mature OM, indicating rapid and early sulfidization of an original OM-rich matrix. The presence of coherent OM strands and filaments entombed within this nanoporous pyrite, and $\delta^{13}C$ values that lie within the range of biological OM, are consistent with an origin from microbial communities, thus providing compelling evidence for the biologically mediated formation of the Dresser Formation stromatolites.

ACKNOWLEDGMENTS

We acknowledge the facilities and the technical assistance of the Microscopy Australia research facility at the Centre for Microscopy, Characterization and Analysis, University of Western Australia. This study was supported by the Australian Research Council (ARC) Centre of Excellence for Core to Crust Fluid Systems (www.ccfs.mq.edu.au).

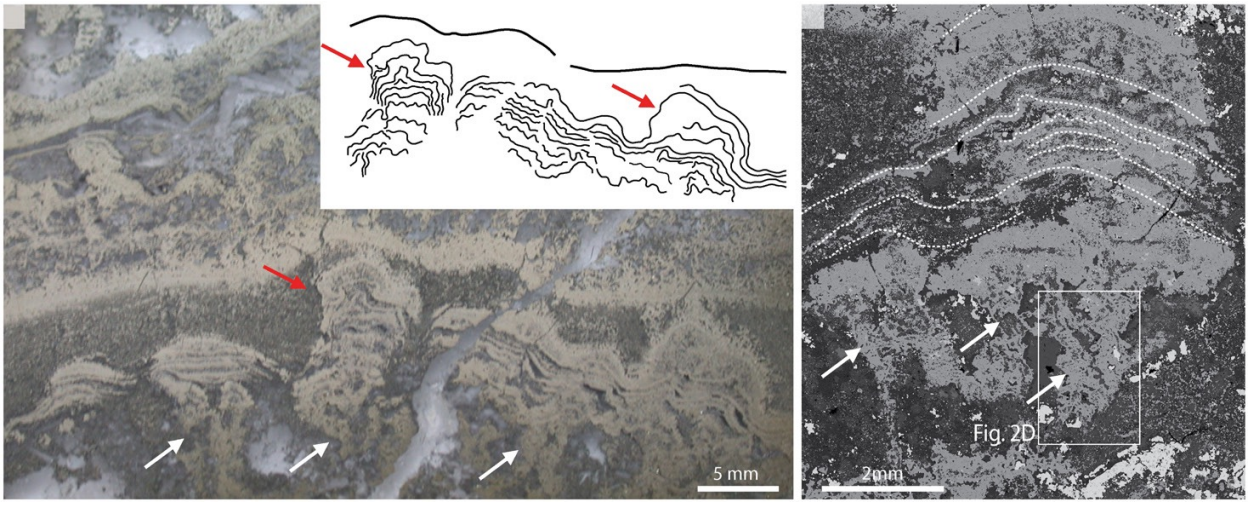

Figure 1. Photomicrograph and scanning electron microscope (SEM) images of sulfidized Dresser Formation (Pilbara Craton, Western Australia) stromatolites. (A) Photomicrograph of stromatolites in chert-dolomite of sample S1. Stromatolite textures range from upward-broadening and/or upward-branching digitate structures (white arrows), to wavy and wrinkly laminae that are occasionally arranged in a columnar fashion (red arrow); see also Fig. DR2a (see footnote 1). The inset shows a schematic drawing of stromatolite lamination. Note the steep (near vertical) inclination of some laminae at the margins of stromatolite columns, as well as the thickening of laminae at flexure crests (red arrows). (B) Backscattered electron (BSE) image of stromatolites in chert-dolomite of sample S1 (see imaging location in Fig. DR2a). Stromatolite textures range from wavy and wrinkly laminae (white lines), to upward-broadening and/or upward-branching digitate structures (white arrows); compare with A. Mineralogy is gauged from brightness differences and supported by EDS analysis: white—barite; light gray—sulfide (mainly pyrite ± sphalerite); dark gray—quartz and dolomite.

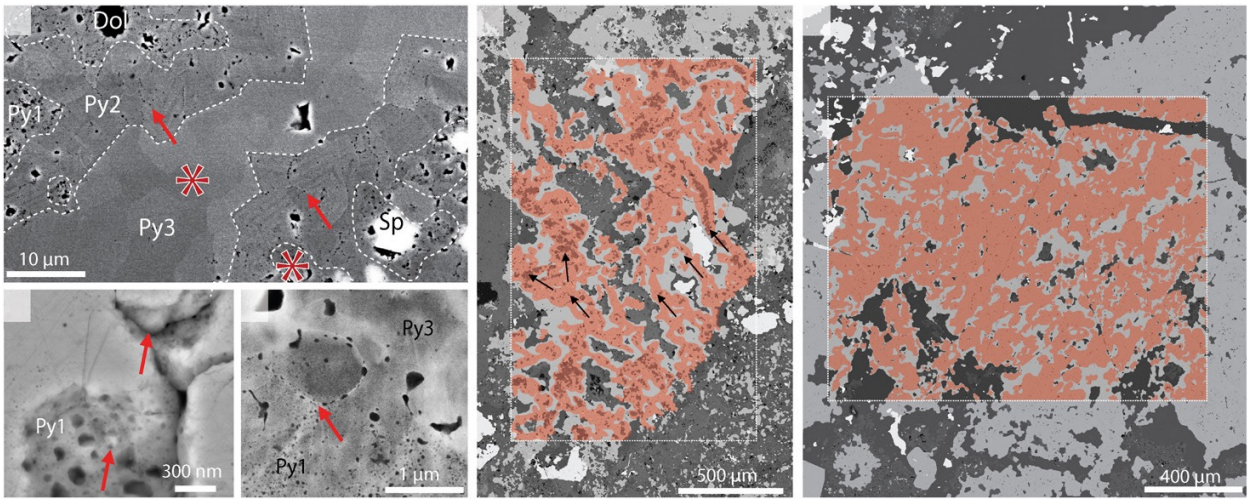

Figure 2. Pyrite textures in the Dresser Formation (Pilbara Craton, Western Australia) stromatolites. (A) Backscattered electron (BSE) image of representative pyrite assemblages, ranging from irregular (Py1) to zoned (Py2) nanoporous pyrite, to later overgrowths of non-porous, massive pyrite (Py3). Fine-scale zonation within Py2 is indicated (red arrows). Note the grains of dolomite (Dol) and sphalerite (Sp) that are associated with Py1 and Py2. See the nanoscale secondary ion mass spectrometry (NanoSIMS) ion maps of $^{58}Ni^{+}$, $^{16}O^{-}$, $^{12}C^{-}$ and $^{26}CN^{-}$ (Figs. 3A–3D). Asterisks indicate the locations of Raman spectroscopy analyses (Figs. 3E and 3F). (B) Image of irregular nano-porous pyrite (Py1), hosting anhedral to rounded pyrite grains (red arrows). (C) Dark-field scanning transmission electron microscopy (STEM) image of a rounded pyrite grain that is mantled by nanoporous pyrite (see the imaging location in Fig. DR3b [see footnote 1]). (D, E) Image of digitate stromatolites and a sulfidized stromatolite layer (see imaging locations in Figure 1B, and in Figure DR2c). The distributions of Py1 – Py2 assemblages are outlined in red. Black arrows in D indicate the putative growth orientation of vertical, locally upward-branching and/or upward-broadening patterns of Py1 and Py2.

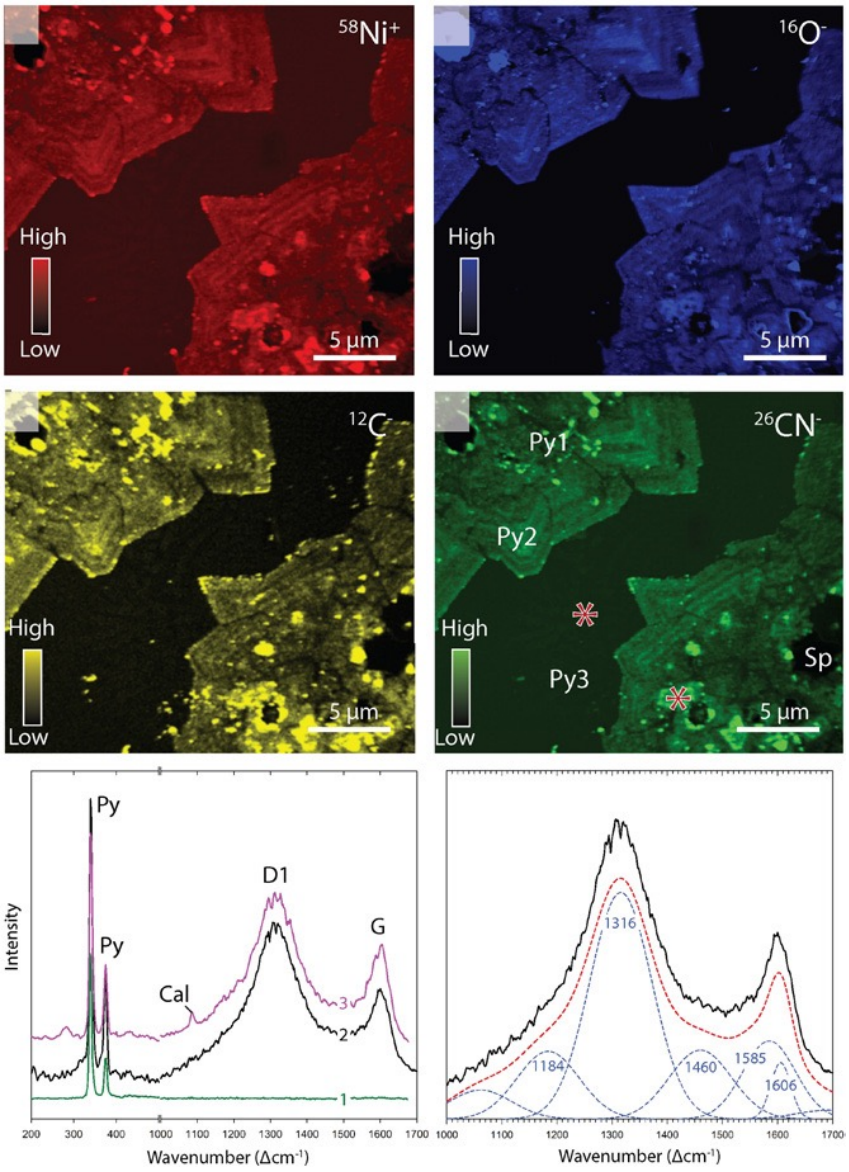

Figure 3. Nanoscale secondary ion mass spec- trometry (NanoSIMS) ion maps and Raman spectroscopy analyses of organic matter (OM) in pyrite of the Dresser For- mation (Pilbara Craton, Western Australia) stromatolites. (A–D) Ion maps of $^{58}Ni^{+}$, $^{16}O^{-}$, $^{12}C^{-}$ and $^{26}CN^{-}$ in pyrite (see the analysis locations in Fig. 2A). The asterisks indicate the locations of Raman spectroscopy analyses in E–F. (E) Raman spectra of non–porous, massive pyrite, and OM-rich nano-porous pyrite (1 and 2, respectively; see the anal- ysis locations in D, and a calcified OM strand (3; see the analysis location in Fig. 4B). Analysis 3 was done on finely striated OM away from discernible cal- cite grains. In analyses 2 and 3, the high intensity of the disorder-induced 'D1' (~1315 ⊗cm^{-1}) band relative to the order-induced 'G' (~1600 ⊗cm^{-1}) band indicates that the OM exhibits a high degree of structural disorder. (F) Deconvolution of spec- trum 2 in E, indicating overlaps of D1 (~1316 ⊗cm^{-1}) and G (~1585 ⊗cm^{-1}) with disorder–induced 'D2' (~1606 ⊗cm^{-1}), 'D3' (~1460 ⊗cm^{-1}), and 'D4' (~1184 ⊗cm^{-1}) bands. The cumulative fit is indicated by red dashed line. Cal—Raman band of calcite; Py—Raman bands of pyrite; Py1—irregular nano-porous pyrite; Py2—zoned nano-porous pyrite; Py3—non-porous, massive pyrite; Sp—sphalerite.

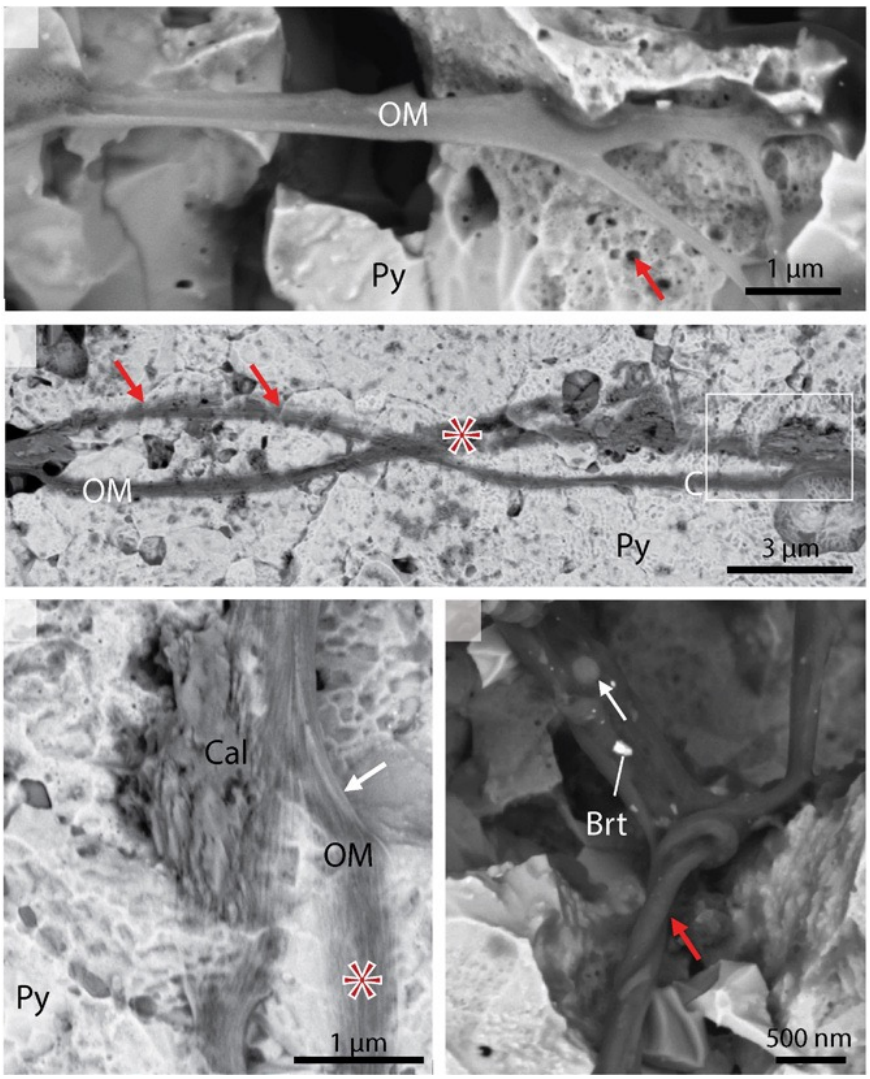

Figure 4. Organic matter strands and filaments in pyrite of the Dresser For- mation (Pilbara Craton, Western Australia) stromatolites. (A) Back- scattered electron (BSE) image of a branched organic matter (OM) strand that is embedded in nano- porous pyrite (red arrow). (B,C) Coher- ent OM strands that traverse pyrite pseudo- grain boundaries (red arrows in B). Note the axial arrangement and the striated texture of the OM strands (white arrow in C). Partial calcification of OM is indicated by inti- mately associated calcite grains (Cal). In addition, Raman spectroscopy analysis of OM (asterisk in B) away from discernible calcite grains shows cal- cite bands (Fig. 3E), and energy dispersive X-ray spectroscopy (EDS) anal- ysis (asterisk in C) shows subtle enrichments of Ca and O (see Fig. DR6a [see footnote 1]). These observations indicate that the OM strands are partially replaced by nanoscopic calcite, whose small particle size may be not readily discernible and distinguishable in BSE imagery. See for these strands the Raman spectroscopy map of OM in Figure. DR7. (D) Twisted filament bundle (red arrow) containing barite (Brt) and quartz or calcite grains (white arrow). See the EDS analyses of this filament bundle in Fig. DR6b. All images in this figure panel were acquired on nitric acid-etched surfaces.

REFERENCES CITED

Allwood, A.C., Grotzinger, J.P., Knoll, A.H., Burch, I.W., Anderson, M.S., Coleman, M.L., and Kanik, I., 2009, Controls on development and diversity of Early Archean stromatolites: Proceedings of the National Academy of Sciences of the United States of America, v. 106, p. 9548–9555, https:// doi.org/10.1073/pnas.0903323106.

Awramik, S.M., and Grey, K., 2005, Stromatolites: Biogenicity, biosignatures, and bioconfu- sion: Proceedings of SPIE, v. 5906, p. 5906P- 1–5906P-9, https://doi.org/10.1117/12.625556.

Buick, R., and Dunlop, J.S.R., 1990, Evaporitic sedi- ments of Early Archaean age from the Warra- woona Group, North Pole, Western Australia: Sedimentology, v. 37, p. 247–277, https://doi .org/10.1111/j.1365-3091.1990.tb00958.x.

Buick, R., Dunlop, J.S.R., and Groves, D.I., 1981, Stro- matolite recognition in ancient rocks: An appraisal of irregularly laminated structures in an Early Ar- chaean chert-barite unit from North Pole, Western Australia: Alcheringa, v. 5, p. 161–181, https://doi .org/10.1080/03115518108566999.

Cosmidis, J., and Templeton, A.S., 2016, Self–assembly of biomorphic carbon/sulfur microstructure in sul- fidic environments: Nature Communications, v. 7, p. 12812, https://doi.org/10.1038/ncomms12812.

Cui, H., Kitajima, K., Spicuzza, M.J., Fournelle, J.H., Denny, A., Ishida, A., Zhang, F., and Valley, J.W., 2018, Questioning the biogenicity of Neoprotero- zoic superheavy pyrite by SIMS: The American Mineralogist, v. 103, p. 1362–1400, https://doi .org/10.2138/am-2018-6489.

Djokic, T., Van Kranendonk, M.J., Campbell, K.A., Walter, M.R., and Ward, C.R., 2017, Earliest signs of life on land preserved in ca. 3.5 Ga hot spring deposits: Nature Communications, v. 8, p. 15263, https://doi.org/10.1038/ncomms15263.

Dunlop, J.S.R., and Buick, R., 1981, Archaean epi- clastic sediments derived from mafic volcanics, North Pole, Pilbara Block, Western Australia: Geological Society of Western Australia Special Publication, v. 7, p. 225–233.

Grotzinger, J.P., and Knoll, A.H., 1999, Stromato- lites in Precambrian carbonates: Evolutionary mileposts or environmental dipsticks?: Annual Review of Earth and Planetary Sciences, v. 27, p. 313–358, https://doi.org/10.1146/annurev. earth.27.1.313.

Grotzinger, J.P., and Rothman, D.H., 1996, An abiotic model for stromatolite morphogen- esis: Nature, v. 383, p. 423–425, https://doi .org/10.1038/383423a0.

Groves, D.I., Dunlop, J.S.R., and Buick, R., 1981, An early habitat of life: Scientific American, v. 245, p. 64–73, https://doi.org/10.1038/scientificam- erican1081-64.

Harris, L.V., Hutchinson, I.B., Ingley, R., Marshall, C.P., Olcott Marshall, O., and Edwards, H.G.M., 2015, Selection of portable spectrometers for plan- etary exploration: A comparison of 532 nm and 785 nm Raman Spectroscopy of reduced carbon in Archean cherts: Astrobiology, v. 15, p. 420–429, https://doi.org/10.1089/ast.2014.1220.

Lowe, D.R., 1994, Abiological origin of described stromatolites older than 3.2 Ga: Geology, v. 22, p. 387–390, https://doi.org/10.1130/0091-7613(1994)022<0387:AOODSO>2.3.CO;2.

MacLean, L.C.W., Tyliszczak, T., Gilbert, P.U.P.A., Zhou, D., Pray, T.J., Onstott, T.C., and Southam, G., 2008, A high-resolution chemical and struc- tural study of framboidal pyrite formed within a low-temperature bacterial biofilm: Geobiology, v. 6, p. 471–480, https://doi.org/10.1111/j.1472- 4669.2008.00174.x.

McCollom, T.M., and Seewald, J.S., 2006, Carbon iso- tope composition of organic compounds produced by abiotic synthesis under hydrothermal conditions: Earth and Planetary Science Letters, v. 243, p. 74– 84, https://doi.org/10.1016/j.epsl.2006.01.027.

McLoughlin, N., Wilson, L.A., and Brasier, M.D., 2008, Growth of synthetic stromatolites and wrinkle structures in the absence of microbes – implications for the early fossil record: Geobi- ology, v. 6, p. 95–105, https://doi.org/10.1111/ j.1472-4669.2007.00141.x.

Morag, N., Williford, K.H., Kitajima, K., Philippot, P., Van Kranendonk, M.J., Lepot, K., Thomazo, C., and Valley, J.V., 2016, Microstructure-specific carbon isotopic signatures of Om from ~ 3.5 Ga cherts of the Pilbara Craton support a biologic ori- gin: Precambrian Research, v. 275, p. 429–449, https://doi.org/10.1016/j.precamres.2016.01.014.

Neveu, M., Hays, L.E., Voytek, M.A., New, M.H., and Schulte, M.D., 2018, The ladder of life detec- tion: Astrobiology, v. 18, p. 1375–1402, https:// doi.org/10.1089/ast.2017.1773.

Otálora, F., Mazurier, A., García–Ruiz, J.M., Van Kranendonk, M.J., Kotopoulou, E., El Albani, A., and Garrido, C.J., 2018, A crystallographic study of crystalline casts and pseudomorphs from the 3.5 Ga Dresser Formation, Pilbara Craton (Australia): Journal of Applied Crystallography, v. 51, p. 1050–1058, https://doi.org/10.1107/ S1600576718007343.

Planavsky, N., Reid, R.P., Lyons, T.W., Myshrall, K.L., and Visscher, P.T., 2009, Formation and diagenesis of modern marine calcified Cyano-bacteria: Geobiology, v. 7, p. 566–576, https://doi .org/10.1111/j.1472-4669.2009.00216.x.

Riding, R., 2000, Microbial carbonates: The geological record of calcified bacterial-algal mats and bio- films: Sedimentology, v. 47, p. 179–214, https:// doi.org/10.1046/j.1365-3091.2000.00003.x.

Schopf, J.W., Kudryavtsev, A.B., Czaja, A.D., and Tripathi, A.B., 2006, Evidence of Archean life: Stromatolites and microfossils: Precam- brian Research, v. 158, p. 141–155, https://doi .org/10.1016/j.precamres.2007.04.009.

Shen, Y., Buick, R., and Canfield, D.E., 2001, Isoto- pic evidence for microbial sulphate reduction in the early Archaean era: Nature, v. 410, p. 77–81, https://doi.org/10.1038/35065071.

Shen, Y.N., Farquhar, J., Masterson, A., Kaufman, A.J., and Buick, R., 2009, Evaluating the role of microbial sulfate reduction in the early Archean using quadruple sulfur isotope systematics: Earth and Planetary Science Letters, v. 279, p. 383–391, https://doi.org/10.1016/j.epsl.2009.01.018.

Sprachta, S., Camoin, G., Golubic, S., and Le Cam- pion, T., 2001, Microbialites in a modern la- goonal environment:nature and distribution, Tikehau atoll (French Polynesia): Palaeogeog- raphy, Palaeoclimatology, Palaeoecology, v. 175, p. 103–124, https://doi.org/10.1016/S0031-0182(01)00388-1.

Terabayashi, M., Masuda, Y., and Ozawa, H., 2003, Archaean ocean floor metamorphism in the North Pole area, Pilbara Craton, Western Australia: Pre- cambrian Research, v. 127, p. 167–180, https:// doi.org/10.1016/S0301-9268(03)00186-4.

Ueno, Y., Isozaki, Y., Yurimoto, Y., and Maruyama, S., 2001, Carbon isotopic signatures of individual Archean microfossils (?) from Western Australia: International Geology Review, v. 43, p. 196–212, https://doi.org/10.1080/00206810109465008.

Ueno, Y., Ono, S., Rumble, D., and Maruyama, S., 2008, Quadruple sulfur isotope analysis of ca. 3.5 Ga Dresser Formation: New evidence for micro- bial sulfate reduction in the early Archean: Geo- chimica et Cosmochimica Acta, v. 72, p. 5675– 5691, https://doi.org/10.1016/j.gca.2008.08.026.

Van Kranendonk, M.J., 2006, Volcanic degassing, hydrothermal circulation and the flourishing of early life on Earth: A review of the evidence from c. 3490–3240 Ma rocks of the Pilbara Super- group, Pilbara Craton, Western Australia: Earth- Science Reviews, v. 74, p. 197–240, https://doi .org/10.1016/j.earscirev.2005.09.005.

Van Kranendonk, M.J., 2011, Stromatolite morphol- ogy as an indictor of biogenicity for Earth's old- est fossils from the 3.5–3.4Ga Pilbara Craton, Western Australia, *in* Reitner, J., Queric, N.-V., and Arp, G., eds., Advances in Stromatolite Geobiology: Berlin, Springer: Lecture Notes in Earth Sciences 131, p. 537–554, https://doi .org/10.1007/978-3-642-10415-2_32.

Van Kranendonk, M.J., and Pirajno, F., 2004, Geo- chemistry of metabasalts and hydrothermal alter- ation zones associated with c. 3.45 Ga chert and barite deposits: implications for the geological setting of the Warrawoona Group, Pilbara Cra- ton, Australia: Geochemistry Exploration Envi- ronment Analysis, v. 4, p. 253–278, https://doi .org/10.1144/1467-7873/04-205.

Van Kranendonk, M.J., Philippot, P., Lepot, K., Bodor- kos, S., and Pirajno, F., 2008, Geological set- ting of Earth's oldest fossils in the ca. 3.5 Ga Dresser Formation, Pilbara Craton, Western Aus- tralia: Precambrian Research, v. 167, p. 93–124, https://doi.org/10.1016/j.precamres.2008.07.003.

Wacey, D., Kilburn, M.R., Saunders, M., Cliff, J.B., Kong, C., Liu, A.G., Matthews, J.J., and Brasier, M.D., 2015, Uncovering framboidal pyrite bioge- nicity using nano-scale CN_{org} mapping: Geology, v. 43, p. 27–30, https://doi.org/10.1130/G36048.1.

Wacey, D., Saunders, M., Cliff, J., Kilburn, M.R., Kong, C., Barley, M.E., and Brasier, M.D., 2014, Geochemistry and nano-structure of a putative ~3240 million-year-old black smoker biota, Sulphur Springs Group, Western Australia: Pre- cambrian Research, v. 249, p. 1–12, https://doi .org/10.1016/j.precamres.2014.04.016.

Walter, M.R., 1983, Archean stromatolites: Evidence of the Earth's earliest benthos, *in* Schopf, J.W., ed., Earth's Earliest Biosphere: Its Origin and Evolution: Princeton, New Jersey, Princeton University Press, p. 187–213.

Walter, M.R., Buick, R., and Dunlop, J.S.R., 1980, Stromatolites 3,400–3,500 Myr old from the North Pole area, Western Australia: Nature, v. 284, p. 443–445, https://doi.org/10.1038/284443a0.